Shear behavior of prestressed steel-fiber-reinforced concrete hollow-core slabs

Vasily S. Dudnik, Lyle R. Milliman, and Gustavo J. Parra-Montesinos

- An experimental study was conducted to evaluate the effect of steel fibers on the shear strength of prestressed concrete hollow-core slabs.
- The main variables investigated were fiber volume fraction, slab thickness, and shear span–to–depth ratio.
- The addition of steel fibers to 16 in. (410 mm) thick hollow-core slabs led to an increase in shear strength between approximately 55% and 90% compared to that of concrete hollow-core slabs that do not contain fibers.

Precast, prestressed concrete hollow-core slabs are used in residential and office construction due to their light weight, economy, and rapid deployment. These structural members are typically manufactured through either an extrusion or a slip-form process. A nearly zero-slump concrete is used in extruded hollow-core slabs, while a slightly more workable concrete is used during a slip-form manufacturing process. In either case, however, the use of traditional shear reinforcement is not feasible, which limits the design shear strength of the member to that assumed to be provided by the concrete.

Hawkins and Ghosh[1] evaluated the shear strength of hollow-core slabs manufactured by three different suppliers and with overall thicknesses of 12.5, 14.5, 15, and 16 in. (318, 368, 380, and 410 mm). All 15 and 16 in. thick slabs, which were manufactured by two different suppliers, exhibited web-shear failures at shear forces between 0.53 and 1.02 of the calculated nominal web-cracking shear strength V_{cw}, according to the 2005 edition of the American Concrete Institute's (ACI's) *Building Code Requirements for Structural Concrete (ACI 318-05) and Commentary (ACI 318R-05)*.[2] The same expression for calculating the nominal web-cracking shear strength is used in the 2014 edition of ACI 318.[3] Hawkins and Ghosh[1] thus concluded that a reduction in the design web-cracking shear strength of units thicker than 12.5 in. seems warranted. This conclusion led to the introduction in ACI 318-08[4] of a 50% reduction in the design web-

cracking shear strength for hollow-core slabs thicker than 12.5 in. This reduction is also applied in ACI 318-14.

The effect of depth on the shear strength of hollow-core slabs was also recently evaluated by Palmer and Shultz,[5] who conducted an experimental study in which hollow-core slabs from two different suppliers and with depths of 12, 16, and 20 in. (300, 410, and 510 mm) were tested to failure. One supplier used a slip-form process for all 16 in. thick slabs, while the other used an extrusion process to manufacture all of the slabs. The span-to-depth ratio a/d ranged between 2.5 and 4.0. Test results indicated substantial variations in shear strength and strand end slip among suppliers. Calculated web-shear strengths for the 16 and 20 in. deep slabs according to ACI 318-14 were found to be overly conservative in some cases. Increases in strand end slip were found to be consistent with decreases in web-cracking shear strength.

Because bar-type reinforcement cannot be used to increase shear strength in hollow-core slabs constructed through an extrusion or slip-form process, the use of discontinuous deformed steel fibers as shear reinforcement was evaluated in this project. Fiber reinforcement may increase shear strength by providing post-cracking diagonal tensile resistance and controlling the opening of cracks, which leads to increased aggregate interlock. Fiber reinforcement may also have the potential to increase shear strength in end regions of prestressed concrete members by reducing prestressing strand transfer length because research has shown that fiber reinforcement enhances bond between prestressing strands and the surrounding concrete.[6,7] Because the web-cracking shear capacity V_{cw} increases with an increase in prestressing force, a reduction in transfer length would increase the amount of prestressing force and, thus, web-shear strength, near the end of the member.

The main objective of this research was to experimentally investigate the effect of steel fiber reinforcement on the shear behavior of prestressed hollow-core slabs. For this purpose, shear tests on 12 and 16 in. (300 and 410 mm) thick hollow-core slabs were conducted. The concrete used in all slabs (with or without fibers) had the same proportions, except for the presence of hooked steel fibers, which were used in volume fractions of 0.38%, 0.50%, or 0.76% (50, 66, or 100 lb/yd^3 [30, 39, or 59 kg/m^3]).

Shear provisions in ACI 318-14 for prestressed hollow-core slabs

ACI 318-14 provides two methods for calculating the concrete nominal shear strength in prestressed concrete members, an approximate or simplified method (section 22.5.8.2) and a more refined or elaborate method (section 22.5.8.3). According to section 22.5.8.2 of ACI 318-14, the shear strength provided by the concrete V_c should be the least of Eq. (1) through (3):

$$\left(0.6\lambda\sqrt{f_c'} + 700\frac{V_u d}{M_u}\right)b_w d \quad (1)$$

$$\left(0.6\lambda\sqrt{f_c'} + 700\right)b_w d \quad (2)$$

$$5\lambda\sqrt{f_c'}\, b_w d \quad (3)$$

but not less than Eq. (4):

$$2\lambda\sqrt{f_c'}\, b_w d \quad (4)$$

where

λ = factor that accounts for the reduced tensile strength of lightweight concrete compared with normalweight concrete = 1.0 for normalweight concrete

f_c' = specified concrete compressive strength

V_u = factored shear at the section considered

M_u = factored moment that occurs simultaneously with the factored shear V_u at the section considered

b_w = web width

A more refined method for calculating the nominal shear strength of prestressed concrete members based on research conducted at the University of Illinois[8–10] is given in section 22.5.8.3. In this method, V_c is the lesser of the shear corresponding to flexural-shear cracking V_{ci} and that corresponding to web-shear cracking V_{cw}. The flexure shear strength V_{ci} is taken as the greater of Eq. (5) and (6) (ACI 318-14 section 22.5.8.3.1).

$$V_{ci} = 0.6\lambda\sqrt{f_c'}b_w d_p + V_d + \frac{V_i M_{cre}}{M_{max}} \quad (5)$$

$$V_{ci} = 1.7\lambda\sqrt{f_c'}b_w d_p \quad (6)$$

where

d_p = distance from the extreme compression fiber to the centroid of the prestressing steel (not less than 0.8 times the member height h)

V_d = unfactored shear force due to dead load

V_i = factored shear force at the section under consideration due to externally applied load (that is, load other than unfactored dead load)

M_{cre} = moment causing flexural cracking due to externally applied loads, calculated as Eq. (7)

M_{max} = maximum factored moment at the section due to externally applied loads and concurrent with V_i

$$M_{cre} = \frac{I}{y_t}\left(6\lambda\sqrt{f_c'} + f_{pe} - f_d\right) \quad (7)$$

where

I = section moment of inertia

y_t = distance from the centroid of the section to the extreme precompressed fiber

f_{pe} = stress in the concrete in the extreme precompressed fiber due to the effective prestressing force

f_d = stress in the concrete in the extreme precompressed fiber due to the unfactored dead load

Web-shear cracking strength V_{cw} is calculated as Eq. (8) (ACI 318-14 section 22.5.8.3.2).

$$V_{cw} = \left(3.5\lambda\sqrt{f_c'} + 0.3f_{pc}\right)b_w d_p + V_p \quad (8)$$

where

f_{pc} = compressive stress in the concrete at the centroid of the section due to the effective prestressing force

V_p = vertical component of the effective prestressing force at the section considered

Alternatively, ACI 318-14 allows the calculation of V_{cw} as the shear required to produce a principal tensile stress at the centroidal axis of the section of $4\lambda\sqrt{f_c'}$. When the centroidal axis of the section is in the flange, however, the principal tensile stress should be calculated at the intersection of the web and flange.

ACI 318-14 section 7.4.3.2 requires that the first critical section be taken at a distance $h/2$ from the face of the support for cases in which the load and support conditions are such that

- any distributed load between the support and the first critical section can be transferred directly to the support through diagonal compression, and
- no concentrated forces are applied over this region.

Yang[11] recommended taking the first critical section at the intersection of the narrowest web width of the hollow-core slab and the line from the center of support at an angle β of 35 degrees with the bottom surface of hollow-core slab. β is the angle with the longitudinal axis of the line connecting the center of support and intersection between the narrowest width of the web and the first critical section according to Yang's model. Hawkins and Ghosh[1] also found evidence, based on test results, that the location of the first critical section is a function of the geometry of the hollow-core slab.

ACI 318-14 section 7.6.3.1 requires the use of minimum shear reinforcement in hollow-core flexural members with depths greater than 12.5 in. (318 mm) wherever V_u exceeds $0.5\phi V_{cw}$, where ϕ is the strength reduction factor equal to 0.75. Because the process used to manufacture hollow-core units does not typically allow the use of bar-type shear reinforcement in the webs of the units, this requirement effectively reduces the design shear strength by 50% for deep hollow-core flexural members. For shallower members, no shear reinforcement is required wherever $V_u \le \phi V_c$.

Steel fibers as shear reinforcement

Extensive research on the use of steel fibers to increase the shear strength of reinforced concrete members has been conducted since the late 1960s. A summary of test data reported in the literature can be found in Parra-Montesinos.[12] The data indicate significant increases in shear strength when deformed steel fibers are used in volume fractions of 0.5% or greater. However, research on the use of fiber reinforcement in hollow-core slabs is rather limited.

Peaston et al.[13] evaluated the shear strength of 8 in. (200 mm) deep hollow-core slabs reinforced with hooked steel fibers in either a 0.5% or 1.0% volume fraction. The specimens were built using an extrusion process that required a slight increase in water content to ensure adequate concrete compaction. Two shear span–to–depth ratios *a*/*d* were evaluated, 2.0 and 2.8. The use of steel fibers was reported to lead to a minor increase in shear strength but a significant enhancement in post-shear-cracking behavior of the slabs with *a*/*d* of 2.8. More-significant increases in shear strength were observed in the slabs with *a*/*d* of 2.0.

Palmer and Schultz[14] reported on the tests of two 16 in. (410 mm) deep slabs reinforced with polypropylene fibers in 0.67% and 1.0% volume fractions. The span-to-depth ratio *a*/*d* was equal to 3.0 for these two specimens. Increases in shear strength of approximately 20% and 40%, respectively, were reported for these two slabs compared with a companion specimen without fibers.

Cuenca and Serna[15] reported on 26 tests of 10.2 in. (259 mm) deep extruded hollow-core slabs with *a*/*d* of 2.3, 4.4, and 8.6. Seven tests were conducted on slabs without fibers, while the other tests were on slabs with a 0.64% or 0.9% volume fraction of hooked steel fibers. Consistent with the findings of other investigators, the addition of steel fibers led to increases in both shear strength and ductility. No major obstacles were reported regarding the use of steel fibers in the manufacturing of extruded hollow-core slabs.

Simasathien and Chao[16] reported on the testing of eight 18 in. (460 mm) deep hollow-core slabs under monotonically increased loading. Six of the slabs were reinforced with hooked steel fibers in a 0.75% volume fraction. The span-to-depth ratio *a*/*d* ranged between 2.0 and 5.1. The slabs were cast as regular beams; no extrusion or slip-form process was used, as is typical for hollow-core slabs. The effect of using a nearly zero-slump concrete with fiber reinforcement was, thus, not evaluated. On average, the fiber-reinforced concrete slabs exhibited shear strengths approximately twice those of the slabs without fibers.

Experimental program

A total of 20 monotonically increased load tests to failure were conducted on prestressed concrete hollow-core slabs, with and without fiber reinforcement, to evaluate the role that fiber reinforcement plays in the shear behavior of these flexural members. Slabs of two different thicknesses, 12 and 16 in. (300 and 410 mm), were tested. Where used, fiber reinforcement consisted of discontinuous hooked steel fibers in volume fractions of either 0.38%, 0.50%, or 0.76% (50, 66, or 100 lb/yd^3 [30, 39, or 59 kg/m^3]). The following sections discuss the properties of the slabs tested, as well as the manufacturing process and test setup used.

Hollow-core slab test specimens

The test hollow-core slabs were cast using an extruder. The specified 28-day concrete compressive strength was 9000 psi (62 MPa), and the target concrete strength at strand release was 3500 psi (24 MPa). Coarse aggregate in the concrete mixture consisted of crushed limestone with a maximum size of ¾ in. (19 mm). The water–cementitious material ratio (0.36) was the same for the mixtures with and without fibers; trial mixtures showed adequate fiber distribution with the same water content. The fibers were added to the mixture simultaneously with the aggregate before any mixing occurred. All fibers used had hooked ends, a length and diameter of 1.18 and 0.022 in. (30.0 and 0.56 mm), respectively, and a specified minimum tensile strength of 160 ksi (1100 MPa). The fibers were delivered in bundles connected by a water-soluble glue that dissolves during concrete mixing to aid in dispersion. Concrete was mixed for 1.5 minutes for both fiber and regular concrete mixtures, which ensured thorough mixing and dispersion of concrete constituents. The concrete was mixed using a 2 yd^3 (1.5 m^3) mixer.

The 12 in. (300 mm) thick hollow-core slabs were reinforced with eight 0.5 in. (13 mm) diameter (total prestressing area A_{ps} of 1.224 in.^{2} [789.7 mm^2]), 270 ksi (1860 MPa) ultimate strength, low-relaxation seven-wire strands (**Fig. 1**). For this strand configuration, the effective depth *d* was 10 in. (254 mm). Each strand had an initial prestress (before concrete casting) of 0.65f_{pu}, (where f_{pu} is the ultimate strength of the prestressing steel) or 175.5 ksi (1210 MPa) for an initial total prestressing force of 215 kip (956 kN). The hollow-core slabs were cast indoors at room temperature, covered, and cured on a heated bed for 12 to 14 hours. The prestressing steel was torch-cut after curing. The hollow-core slabs were then cut to length, removed by crane, and stored outdoors. All 12 in. thick slabs with no fibers or with a fiber volume fraction V_f of 0.38% and 0.5% (50 and 66 lb/yd^3 [30 and 39 kg/m^3]) were cast on the same day. Slabs with V_f of 0.76% (100 lb/yd^3 [59 kg/m^3]) were cast on a single day but at a later date than the other 12 in. thick slabs.

The 16 in. (410 mm) thick slabs were cast in the same

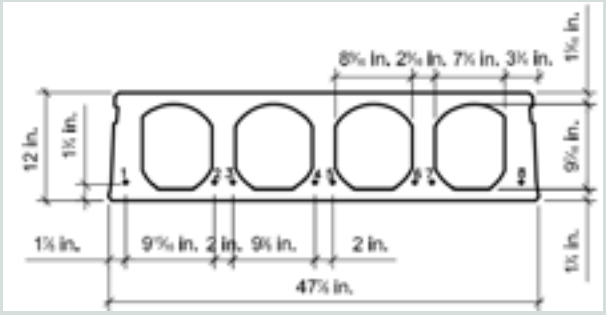

Figure 1. Twelve-inch-thick hollow-core slab cross section. Note: 1 in. = 25.4 mm.

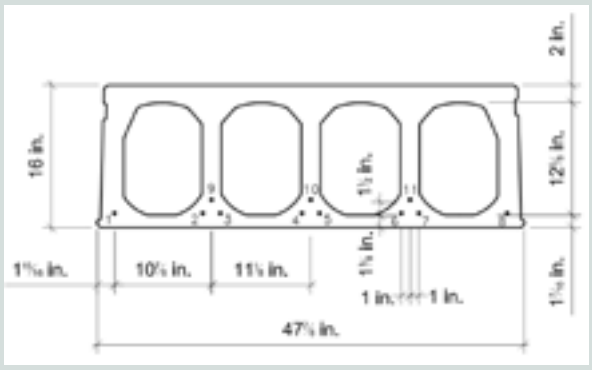

Figure 2. Sixteen-inch-thick hollow-core slab cross section. Note: 1 in. = 25.4 mm.

manner as the 12 in. (300 mm) thick slabs. These slabs were reinforced with eleven strands (two outer 0.5 in. [13 mm] diameter seven-wire strands and nine interior 0.6 in. [15 mm] diameter seven-wire strands) for a total prestressing steel area A_{ps} of 2.259 in.^{2} (1457 mm^2) (**Fig. 2**). For this strand configuration, the effective depth d was 13.9 in. (353 mm). The initial prestress for the strands used in the 16 in. thick hollow-core slabs was also $0.65f_{pu}$ (175.5 ksi [1210 MPa]) for an initial total prestressing force of 396 kip (1760 kN). All 16 in. thick slabs were cast on the same day.

Test setup

Figure 3 shows the general configuration for the hollow-core slab tests. For each test, the pin support was centered at a distance of 1.75 in. (44.5 mm) from the edge of the slab, while a roller support was placed at a distance L from the pin support, where L is the span length in the test specimen. Because both ends of each slab were generally tested, a substantial portion of each test slab cantilevered beyond the roller support so that the shear span to be subsequently tested (that is, the end of the cantilever region) would remain undamaged during the first test. Each test slab was subjected to a concentrated force applied at a distance equal to the shear span a from the center of the pin support through a 1000 kip (4400 kN) actuator.

Figure 4 shows the detail of the pin support. A 64 in. (1630 mm) long W12 × 53 (W310 × 79) section with stiffeners welded at various locations along its length was placed on a steel strong floor. Two 0.76 in. (19 mm) square cross section steel rails were welded on the top of the W section to prevent any lateral displacement of a ¾ in. (19 mm) radius, 54 in. (1370 mm) long steel roller placed between the rails. A 1 × 6 × 48 in. (25 × 150 × 1220 mm) steel plate was placed on top of the steel roller on which a 0.2 × 1.5 × 48 in. (5 × 38 × 1220 mm) multi-monomer plastic bearing pad was placed to mimic support conditions used in actual construction. The outer edge of the bearing pad was located 1 in. away from the edge of the slab (Fig. 4). The details of the roller support were similar to those used in the pin support, except for the lack of steel rails on each side of the roller, which allowed horizontal translation of the roller.

The crosshead of the hydraulic actuator used to apply the concentrated force had a 12 in. (300 mm) diameter circular section. To distribute the applied load over the width of the slab, a spreader beam was placed between the hollow-core slab and the crosshead. A 0.5 × 6 × 48 in. (13 × 150 × 1220 mm) commercial grade 200 neoprene bearing pad was used to distribute the load more evenly from the spreader beam to the slab top surface.

Specimen designation

Three variables were investigated during this experimental program: slab height h, volume fraction of fibers in the concrete matrix V_f, and shear span length a (Fig. 3). With that, a numbering system was used to represent each test conducted. Slab thickness is designated in inches. Fiber volume fraction is designated by a capital letter—A through D—where A corresponds to V_f of 0%, B to V_f of 0.38%, C to V_f of 0.5%, and D to V_f of 0.76%. The letter representing the fiber volume fraction is followed by a number, either 1 or 2, to account for cases in which two nominally identical slabs were cast. The side tested is designated as E or W, which stands for east and west, respectively. Sides were assigned based on the direction in which slabs were cast on the casting bed in the precast concrete plant. The letter corresponding to the side tested is followed by the shear span length. Two different shear span lengths a were tested, 3.0d and 3.5d, where d is the effective depth of the slab. For example, specimen 12-A1-E-3.0d corresponds to a specimen with height of 12 in. (300 mm), no fibers (letter A), first test (number 1), east side (letter E), and a shear span length of 3.0d. **Table 1** lists all 20 tests, along with the dimensions defined in Fig. 3. and the fiber volume fraction V_f used.

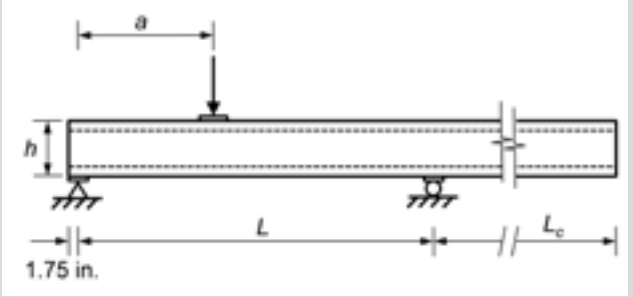

Figure 3. Hollow-core slab test setup. Note: a = length of shear span; h = member height; L = span length in test specimens; L_c = length of cantilever in test specimens. 1 in. = 25.4 mm.

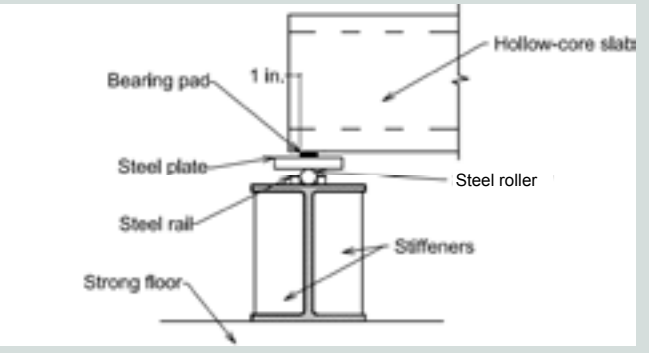

Figure 4. Pin support detail. Note: 1 in. = 25.4 mm.

Table 1. Specimen geometry and calculated and experimental shear strengths

Specimen	h, in.	d, in.	a/d	L, in.	L_c, in.	V_f, %	f_{pc}, psi	f'_c, psi	V_{cw}, kip	V_{ci}, kip	V_{exp}, kip	V_{exp}/V_{cw}
12-A1-E-3.5d	12	10.0	3.5	85	69	0	588	11,140	61.8	70.9	51.8	0.84
12-A1-W-3.5d	12	10.0	3.5	85	69	0	588	11,140	61.8	70.9	52.1	0.84
12-A2-E-3.0d	12	10.0	3.0	80	74	0	588	11,140	61.8	83.2	59.0	0.95
12-A2-W-3.0d	12	10.0	3.0	80	74	0	588	11,140	61.8	83.2	61.0	0.99
12-B1-E-3.5d	12	10.0	3.5	85	69	0.38	588	9060	56.7	68.3	52.5	0.93
12-B1-W-3.5d	12	10.0	3.5	85	69	0.38	588	9060	56.7	68.3	55.8	0.98
12-B2-E-3.0d	12	10.0	3.0	80	74	0.38	588	9060	56.7	80.2	66.4	1.17
12-B2-W-3.0d	12	10.0	3.0	80	74	0.38	588	9060	56.7	80.2	73.7	1.30
12-C1-E-3.5d	12	10.0	3.5	85	69	0.50	588	10,690	60.8	70.4	62.3	1.03
12-C1-W-3.5d	12	10.0	3.5	85	69	0.50	588	10,690	60.8	70.4	65.1	1.07
12-C2-E-3.0d	12	10.0	3.0	80	74	0.50	588	10,690	60.8	82.6	72.0	1.18
12-C2-W-3.0d	12	10.0	3.0	80	74	0.50	588	10,690	60.8	82.6	61.0	1.00
12-D1-W-3.5d	12	10.0	3.5	85	69	0.76	588	7630	52.8	66.2	55.1	1.04
12-D2-E-3.0d	12	10.0	3.0	80	74	0.76	588	7630	52.8	77.9	50.9	0.96
16-A1-E-3.5d	16	13.9	3.5	119	59	0	946	10,520	73.2	112	50.6	0.69
16-A1-W-3.0d	16	13.9	3.0	112	66	0	946	10,520	73.5	133	53.6	0.73
16-C1-E-3.5d	16	13.9	3.5	119	59	0.50	946	10,890	74.2	113	91.3	1.23
16-C1-W-3.0d	16	13.9	3.0	112	66	0.50	946	10,890	74.9	134	99.0	1.33
16-D1-W-3.5d	16	13.9	3.5	119	59	0.76	946	10,320	72.7	112	78.2	1.08
16-D1-E-3.0d	16	13.9	3.0	112	66	0.76	946	10,320	72.9	133	102	1.40

Note: a = length of shear span; d = effective depth = distance from extreme compression fiber to centroid of tension steel; f'_c = concrete compressive strength (specified strength when referring to ACI 318-14, cylinder strength when referring to test results); f_{pc} = compressive stress in the concrete at centroid of cross section due to effective prestressing force; h = member height; L = span length in test specimens; L_c = length of cantilever in test specimens; V_{ci} = nominal flexural-shear cracking strength; V_{cw} = nominal web-cracking shear strength; V_{exp} = peak shear force applied during experiment (excluding specimen self-weight); V_f = fiber volume fraction. 1 in. = 25.4 mm; 1 kip = 4.448 kN; 1 psi = 6.895 kPa.

Test control and instrumentation

All tests were conducted under displacement control on the 1000 kip (4400 kN) actuator crosshead. Displacement of the crosshead was monitored through a linear variable differential transformer. Except for the first slab tested, specimen 12-B2-W-3.0d, the crosshead was moved at a rate of 0.03 in./min (0.8 mm/min). The displacement rate for specimen 12-B2-W-3.0d, alternatively, was controlled manually. Difficulties in manually controlling the loading head led to the use of a uniform displacement rate during all other slab tests. The applied load was monitored through a load cell attached to the crosshead.

A motion capture system was used to track the position of points (markers) on the slab during testing. Specifically, the data acquired from this system were used to determine the deflection of the slab under the load, the state of average strain on one side of the slab along the test shear span, strand slip during testing, and selected average strains at the end region of the interior webs.

Concrete mechanical properties

To evaluate the compressive strength of the mixtures with different fiber volume fractions, 4 × 8 in. (100 × 200 mm) or 6 × 12 in. (150 × 300 mm) cylinders were cast for each concrete mixture and tested in accordance with ASTM C39-12.[17] The cylinders were cast during the production process of the hollow-core slabs; Table 1 lists the concrete compressive strength for all test slabs. The forms were placed on a vibrating table and filled using three to four lifts per test cylinder. After adding each lift, the concrete was compacted for three to four minutes using a 25 lb (110 N), 4 in. (100 mm) diameter compacting cylinder. The cylinders were placed in the quality control laboratory at the precast concrete plant, where they remained for curing, and were later transported to the materials testing laboratory. On the day of testing, the cylinders were demolded and capped with a sulfur compound. Compressive tests were conducted at a load rate of 35 psi/min (240 kPa/min) in accordance with ASTM C39-12.

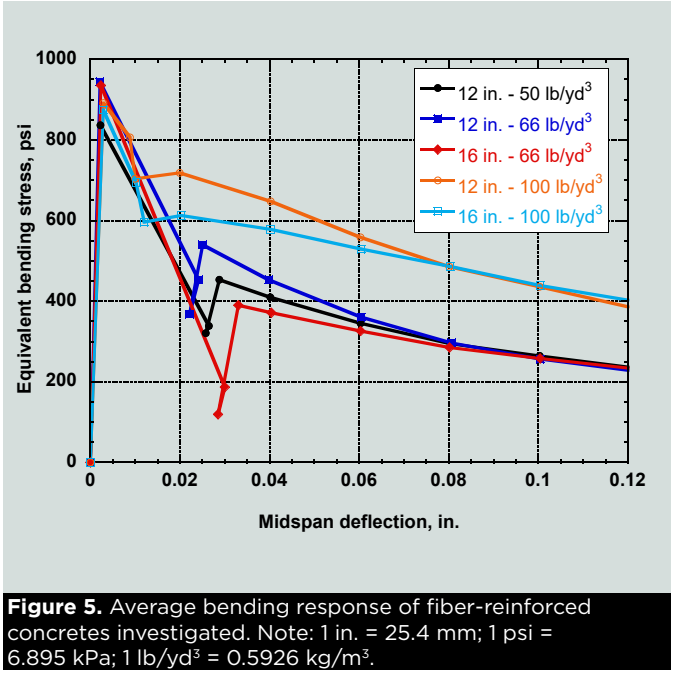

Figure 5. Average bending response of fiber-reinforced concretes investigated. Note: 1 in. = 25.4 mm; 1 psi = 6.895 kPa; 1 lb/yd³ = 0.5926 kg/m³.

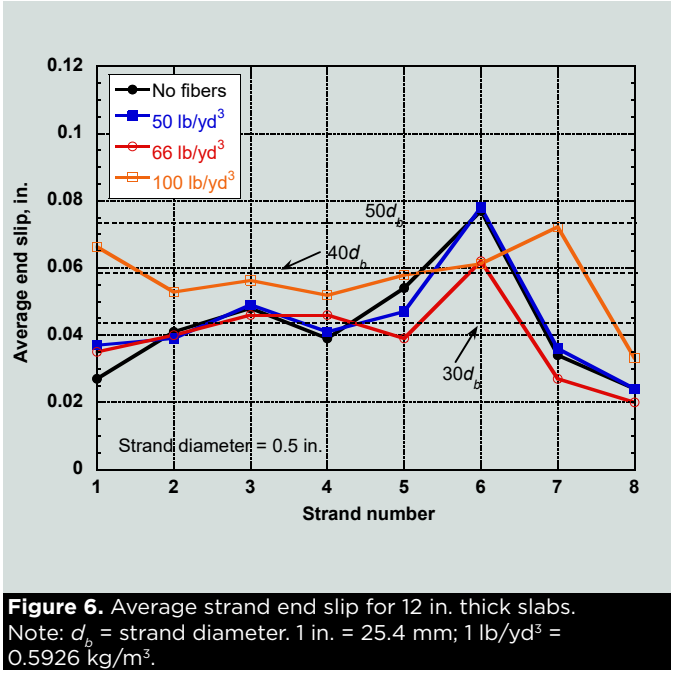

Figure 6. Average strand end slip for 12 in. thick slabs. Note: d_b = strand diameter. 1 in. = 25.4 mm; 1 lb/yd³ = 0.5926 kg/m³.

Flexural behavior of the various fiber-reinforced concretes used was evaluated through four-point bending tests according to ASTM C1609-12.[18] All beams had a 6 × 6 in. (150 × 150 mm) cross section with a span length L of 18 in. (460 mm). Three beams were tested for each material used in the 12 in. (300 mm) thick slabs, while two beams were tested for the materials used in the 16 in. (410 mm) thick slabs. **Figure 5** compares average equivalent bending stress with net midspan deflection response for all materials considered. Equivalent bending stress was calculated assuming an uncracked, linear elastic behavior.

All materials investigated exhibited a deflection-softening response (Fig. 5). Average first cracking strength ranged from about 850 to 950 psi (5.86 to 6.55 MPa). For concretes with fibers in a 0.38% volume fraction (50 lb/yd³ [30 kg/m³]), the average residual strengths at midspan deflections of L/300 and L/150 (0.06 and 0.12 in. [1.5 and 3.0 mm]) were approximately 350 and 230 psi (2.41 and 1.59 MPa), respectively (approximately 40% and 25% of the first cracking strength). Similar residual strengths were observed in the concretes with a 0.50% fiber volume fraction or 66 lb/yd³ (39 kg/m³). Although the fiber content in the two materials was different, the number of fibers crossing the single crack that developed in each beam was nearly the same, which explains the nearly equal residual strengths.

A substantially better behavior was observed in the concretes with a 0.76% fiber volume fraction (100 lb/yd³ [59 kg/m³]). In this case, average residual strengths at midspan deflections of L/300 and L/150 were approximately 550 and 400 psi (3.79 and 2.76 MPa) and roughly 65% and 40% of the first cracking strength, respectively. None of the materials evaluated satisfied the performance criteria specified in ACI 318-14 for use of deformed steel fibers as minimum shear reinforcement in beams (ACI 318-14 section 26.12.5).

Strand end-slip measurement

Strand end slip can be used to estimate transfer length and, thus, the buildup of prestressing force at the end of the member. Due to irregularities on the concrete surface at the end of the hollow-core slab specimens, the end slip for each strand was measured before each test as follows. First, three measurements were made from the surface of a steel plate bearing on the concrete surface to the concrete surrounding the strand (top center, bottom right, bottom left). Then the distance between the steel plate and each wire within the seven-wire strand was measured. The average distance to the concrete surface was subtracted from the average distance to the strand wires to obtain the average end slip for each strand.

Figure 6 shows the average end-slip measurements for the 0.5 in. (13 mm) diameter strands in the 12 in. (300 mm) thick slabs along with expected end slips corresponding to $30d_b$, $40d_b$, and $50d_b$ (where d_b is the strand diameter), assuming a strand stress equal to 95% of the initial stress (that is, 167 ksi [1150 MPa]) and a strand modulus of elasticity of 28,500 ksi (197 GPa). For each strand, values shown correspond to the average value of the slips measured for that particular strand in all 12 in. thick slabs with the same concrete mixture. Strand end slips for each slab specimen can be found elsewhere.[19] The calculated average end slips suggest that the transfer length for a 0.5

in. strand in the 12 in. thick slabs was approximately $30d_b$ to $40d_b$ for most cases, which is considerably less than the $50d_b$ recommended in ACI 318-14. All 12 in. thick slabs were cast on the same day and belonged to the same production line except for those with V_f of 0.76%, which were cast at a later date.

Overall, the presence of fibers did not influence the amount of end slip of strands in the 12 in. (300 mm) thick hollow-core slabs. For the first group of 12 in. thick slabs cast, strand 6 showed consistently higher end slip values; however, the reason for this behavior is not known. The 12 in. thick slabs with V_f of 0.76% (100 lb/yd^3 [59 kg/m^3]) were cast separately, and no single strand experienced a pronounced end slip. Strands in the slabs with V_f of 0.76%, however, experienced the greatest average end slip of all the 12 in. hollow-core slabs. These hollow-core slabs had the poorest concrete compaction, which emphasizes the need to improve workability of concrete with higher fiber volume fractions. In addition, in most cases, the strands with the greatest concrete cover experienced the least end slip. This was most noticeable for exterior strands in both the 12 and 16 in. (410 mm) thick slabs.

Some strands in the 16 in. (410 mm) thick hollow-core slabs exhibited a small decrease in end slip as the presence and amount of fibers increased (**Fig. 7**). This trend was most noticeable for strands 9 through 11 (Fig. 2). All inner strands (strands 2 through 7 and 9 through 11 in Fig. 2) were 0.6 in. (15 mm) diameter strands, while the two outer strands (strands 1 and 8 in Fig. 2) were 0.5 in. (13 mm) in diameter. The transfer length for the 0.6 in. diameter strands was substantially greater than that for the 0.5 in. diameter strands. The observed average end slip suggests that the average transfer length for a 0.6 in.

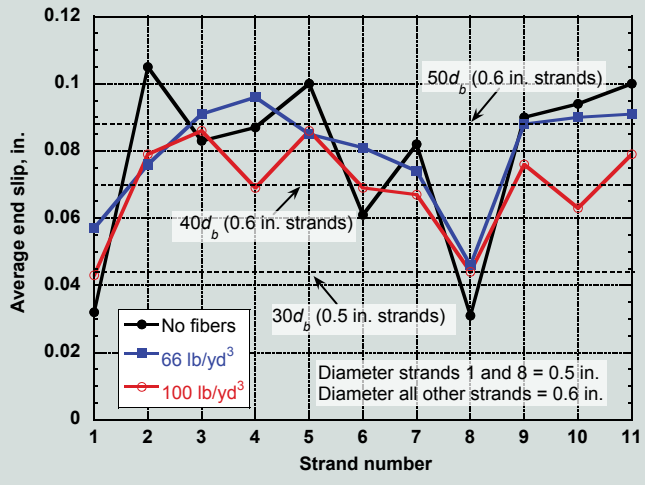

Figure 7. Average strand end slip for 16 in. thick slabs. Note: d_b = strand diameter. 1 in. = 25.4 mm; 1 lb/yd^3 = 0.5926 kg/m^3.

strand in the 16 in. thick slabs was approximately $50d_b$, as recommended in ACI 318-14.

Fiber dispersion

To evaluate the dispersion and quantity of fibers crossing a single plane, the end of each slab test specimen was divided into top flange, bottom flange, and web portions. This allowed a better evaluation of fiber distribution across the depth of the hollow-core slabs. The expected number of fibers per unit area can be calculated by Eq. (9).

$$N = \alpha \frac{V_f}{A_f} \tag{9}$$

where

N = number of fibers crossing a unit area plane

α = fiber orientation factor

A_f = cross-sectional area of a fiber

For a three-dimensional random orientation of fibers, various α values have been reported. Soroushian and Lee[20] compiled an extensive list and reported a range of 0.41 to 0.82.

As a whole, the fibers were well distributed and consistently present throughout all specimens. The hollow-core slabs that met or exceeded the expected fiber count using α of 0.41 were those with the lowest volume fraction V_f of 0.38%. For all other mixtures, the counted fibers totaled between 82% and 106% of the calculated expected value, with the only exception being specimen 16-C1-W-3.0d (16 in. [410 mm] thick hollow-core slab with a fiber content of 66 lb/yd^3 (39 kg/m^3). This hollow-core slab had an on-site cut that prevented counting the fibers in the bottom flange, but the web and top flange contained only 59% of the expected number of fibers per unit area. In general, higher fiber counts per unit area corresponded to the top flange, with slightly lower fibers per unit area corresponding to the web and bottom flange. This suggests a slight fiber alignment in the web and bottom flange toward the vertical direction, which for the case of the web would be consistent with reports in Peaston et al.[13]

Test results

Behavior and shear strength of 12 in. (300 mm) thick hollow-core slabs

Fourteen shear tests were performed on 12 in. (300 mm) thick hollow-core slabs. Slabs with volume fractions of fibers V_f of 0% (no fibers), 0.38%, and 0.5% were tested on both ends, while slabs with V_f of 0.76% were tested only on one end because they had partially filled cores at the

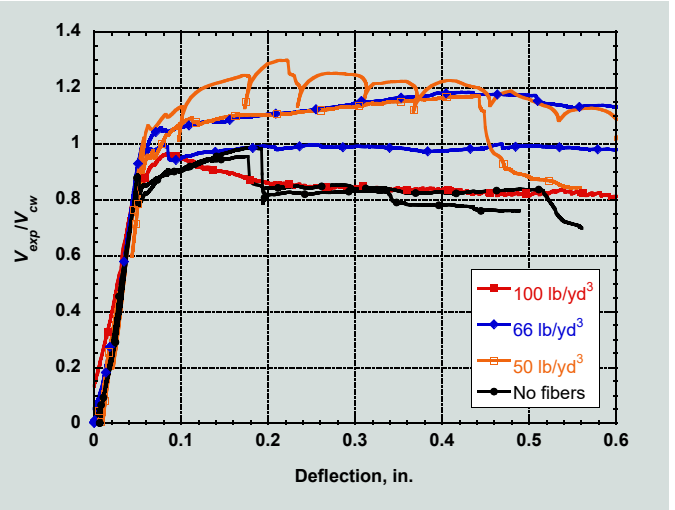

Figure 8. Deflection response versus normalized shear force for 12 in. thick slabs with *a*/*d* of 3.0. Note: *a* = length of shear span; *d* = effective depth; V_{cw} = nominal web-cracking shear strength; V_{exp} = peak shear force applied during experiment (excluding specimen self-weight). 1 in. = 25.4 mm; 1 lb/yd^3 = 0.5926 kg/m^3.

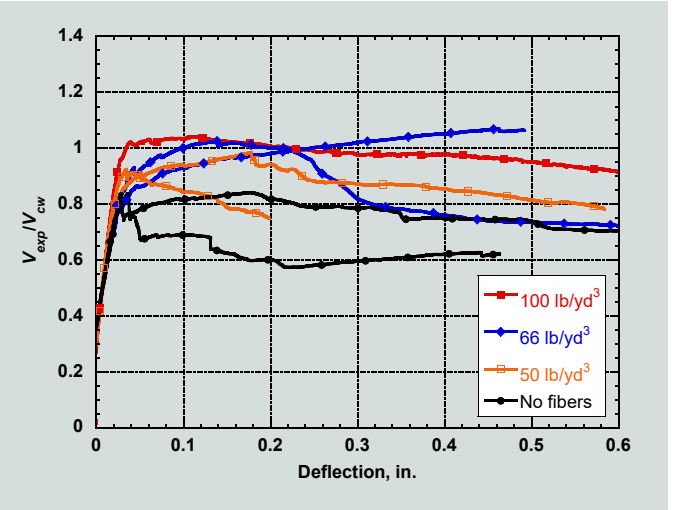

Figure 9. Deflection response versus normalized shear force for 12 in. thick slabs with *a*/*d* ratio = 3.5. *a* = length of shear span; *d* = effective depth; V_{cw} = nominal web-cracking shear strength; V_{exp} = peak shear force applied during experiment (excluding specimen self-weight). 1 in. = 25.4 mm; 1 lb/yd^3 = 0.5926 kg/m^3.

other end. The nominal shear strength of 12 in. slabs was calculated using the more refined method from ACI 318-14 (section 22.5.8.3), as discussed. Table 1 shows the calculated values for V_{ci} and V_{cw}, excluding the slab self-weight. Strength calculations were performed using the concrete compressive strength obtained through cylinder tests, an effective prestress after losses of 150 ksi (1030 MPa), and a transfer length of 50 strand diameters. Calculated values for the slabs with fibers were obtained as for the slabs without fibers. Using a transfer length of 50 strand diameters is slightly conservative because slip measurements indicated a transfer length between 30 and 40 strand diameters (Fig. 6).

The controlling section for V_{cw} corresponded to the first critical section, located at *h*/2 from the face of the support. The controlling section for V_{ci}, alternatively, was the one at *d*/2 from the loading point, which was considered the closest feasible section to the loading point for this failure mode. The shear strength of all 12 in. (300 mm) thick slabs was expected to be governed by the web-cracking shear strength (Table 1).

Web cracking was not necessarily expected at the end of the 12 in. (300 mm) hollow-core slabs, as indicated by results from an approximate calculation of principal tensile stresses assuming an average shear stress over the member effective depth and an equivalent I-shaped cross section. At any section along the shear span for a transfer length of $30d_b$, the principal tensile stress at the junction between the web and the bottom (tension) flange was greater than that at the centroid, with a maximum at a distance *d*/2 from the loading point. Thus it was possible that web-shear cracking developed close to the loading point and not near the support. Also, considering the small difference between V_{cw} and V_{ci} for some of the slabs, combined with the significant variabilities in concrete tensile strength, it was expected that some specimens would exhibit a flexural-shear failure.

Figures 8 and **9** compare the normalized shear force versus load point deflection response for the 12 in. thick hollow-core slabs for *a*/*d* of 3.0 and 3.5, respectively. For easy comparison, the applied shear force has been normalized by the calculated V_{cw}. First inclined cracking is believed to have developed on an interior web, followed by inclined cracking in the exterior webs. Inclined cracking on the exterior webs and/or rapid propagation of an inclined crack, led to a sudden drop in load. Most specimens exhibited a web-shear cracking failure (**Fig. 10**). However, the location of the web-shear crack varied along the shear span, which as discussed previously, was not unexpected. Further, cracking on the outside webs indicated that a few slabs ex-

Figure 10. Web-cracking shear failure for specimen 12-B1-E-3.5d.

hibited what appeared to be a flexural-shear failure mode.

Once diagonal cracking occurred, most 12 in. (300 mm) thick slabs tended to behave as a tied arch, where the applied load traveled to the support through diagonal compression in the concrete, allowing the slab to maintain a large percentage of the peak shear strength or even to sustain additional load. The same arch action effect was noticed in previous shear tests of prestressed concrete members.[21]

Table 1 shows that the two regular concrete slabs (no fibers) tested with an *a*/*d* of 3.5 failed at shear forces slightly less than 85% of the calculated capacity. The regular concrete slabs tested with *a*/*d* of 3.0, alternatively, exhibited shear strengths similar to the calculated strengths. Adding fibers in amounts of 50 and 66 lb/yd^3 (30 and 39 kg/m^3) (V_f equal to 0.38% and 0.50%) led to increases in shear strength of up to 30%. This is attributed to the postcracking tensile strength of the fiber concrete, which allowed the transfer of tensile forces across the diagonal cracks. Slabs with V_f equal to 0.76% showed a lower normalized shear capacity compared with the slabs that had V_f equal to 0.5%, likely due to concrete compaction problems, as discussed previously.

Behavior and strength of 16 in. thick hollow-core slabs

In total, six 16 in. (410 mm) hollow-core slab shear spans were tested. Two shear spans with no fibers, two with V_f equal to 0.5%, and two with V_f equal to 0.76%. Table 1 shows the calculated values for V_{ci} and V_{cw}. For these slabs, V_{ci} was approximately 50% to 80% greater than V_{cw}. Given such a large difference between the two calculated shears, all 16 in. thick slabs were expected to fail by web-shear cracking. Contrary to the 12 in. (300 mm) thick slabs, the maximum calculated principal tensile stress at any section along the shear span occurred at the section centroid, and the controlling value corresponded to the first critical section for shear at *h*/2 from the face of the support.

Table 1 shows that the regular concrete slabs had the lowest shear strength, which was substantially smaller than the calculated V_{cw}. As for the 12 in. (300 mm) thick slabs, shear capacity was calculated using the concrete compressive strength obtained through cylinder tests, a 150 ksi (1030 MPa) effective prestress, and a transfer length of 50 strand diameters. These low shear strengths thus support the 50% reduction in web-cracking shear strength currently applied in ACI 318-14 to hollow-core slabs with depths greater than 12.5 in. (318 mm). The slabs with fiber reinforcement in volume fractions V_f of 0.5% and 0.76% showed substantially greater shear strength, all above the calculated V_{cw} and above $1.2V_{cw}$ for three out of the four shear spans tested.

Figures 11 and **12** compare the normalized shear force versus load point deflection responses for the 16 in. (410 mm) thick hollow-core slabs with *a*/*d* of 3.0 and 3.5, respectively. The substantial increase in shear strength achieved with the addition of hooked steel fibers is evident. In these slabs, no significant arch action was noticed, contrary to the 12 in. (300 mm) thick slabs. This is likely due to the greater transfer length of the 0.6 in. (15

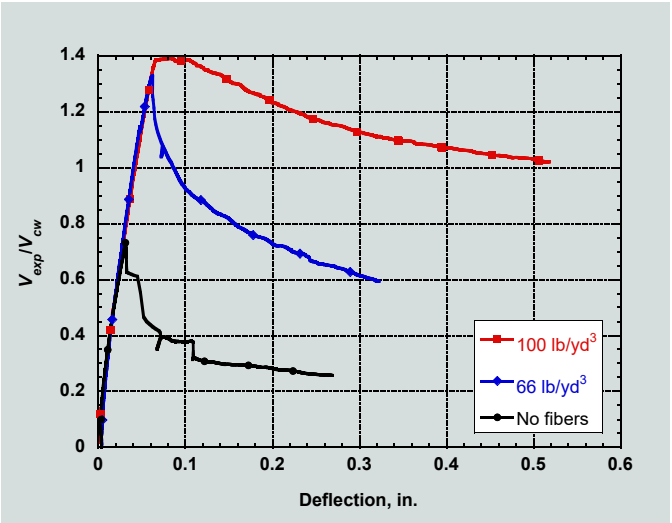

Figure 11. Deflection response versus normalized shear force for 16 in. thick slabs with *a*/*d* of 3.0. *a* = length of shear span; *d* = effective depth; V_{cw} = nominal web-cracking shear strength; V_{exp} = peak shear force applied during experiment (excluding specimen self-weight). 1 in. = 25.4 mm; 1 lb/yd^3 = 0.5926 kg/m^3.

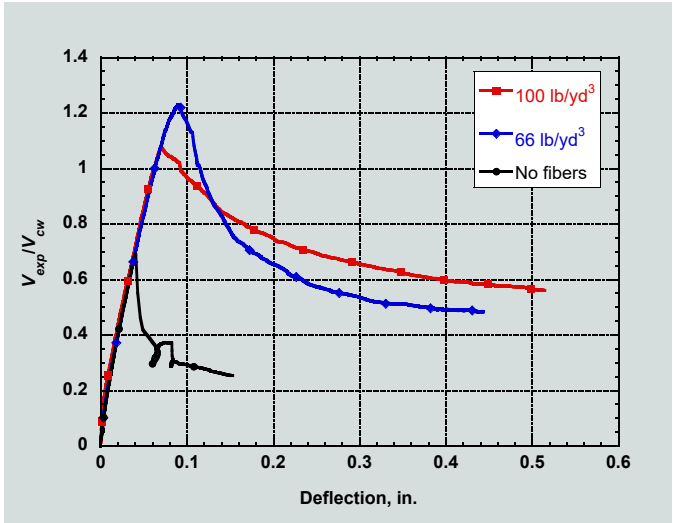

Figure 12. Deflection response vs. normalized shear force for 16 in. thick slabs with *a*/*d* ratio = 3.5. Note: *a* = length of shear span; *d* = effective depth; V_{cw} = nominal web-cracking shear strength; V_{exp} = peak shear force applied during experiment (excluding specimen self-weight). 1 in. = 25.4 mm; 1 lb/yd^3 = 0.5926 kg/m^3.

mm) diameter strands used in the 16 in. thick slabs while the support width remained the same.

All 16 in. (410 mm) thick hollow-core slabs had a horizontal crack on the interior webs propagating from the inclined cracks to the support (**Fig. 13**). This type of horizontal cracking was noted in prestressed concrete members with $\frac{\rho_g E_s}{f'_c}$ ranging between 50 and 60 (where ρ_g is the percentage of longitudinal prestressing steel based on gross area [A_{ps}/A_c, where A_c is the member cross-sectional area]) and a prestressing stress of 120 ksi (830 MPa).[21] The prestress of 120 ksi is lower than that used in this research (175.5 ksi [1210 MPa] initial prestress), but horizontal cracking occurs more readily at higher prestressing forces.[21] The 16 in. thick slabs in this study had high prestress in the interior webs, with $\frac{\rho_g E_s}{f'_c}$ equal to approximately 54, assuming an equivalent I-shaped cross section. The exterior webs, with $\frac{\rho_g E_s}{f'_c}$ equal to approximately 13, did not exhibit horizontal cracking once the inclined crack formed.

Figure 13. Horizontal cracking in interior web of 16 in. (410 mm) thick hollow-core slab (16-A1-W-3.0d).

Effect of fibers on failure progression of 16 in. (410 mm) thick slabs

Steel fibers had a significant effect on the shear strength of the 16 in. (410 mm) thick slabs tested in this investigation. Similar to previous tests of hollow-core slabs without fibers,[5] diagonal cracks in the 16 in. thick slabs first developed in the internal webs. The slabs without fibers failed immediately after the first diagonal cracking due to the inability of the uncracked webs to carry the shear strength loss experienced by the cracked web(s). **Figure 14** shows the relationship between normalized applied shear and principal tensile strains at various locations on both interior and exterior webs of specimen 16-A1-E-3.5d (no fibers). An increase in principal tensile strain in Fig. 14 indicates the formation and opening of a crack. As can be seen in Fig. 14, element W3, E3 (web 3, element 3) was the first to show a sudden increase in strain, indicating that the middle web cracked first. The loss of shear capacity in this web triggered immediate cracking of all subsequent webs, which was accompanied by a rapid loss of strength in the slab.

The behavior of the 16 in. (410 mm) thick steel-fiber-reinforced concrete slabs differed significantly from that of the regular concrete slabs. After the first diagonal cracking, the interior webs of the slabs with steel fibers could carry

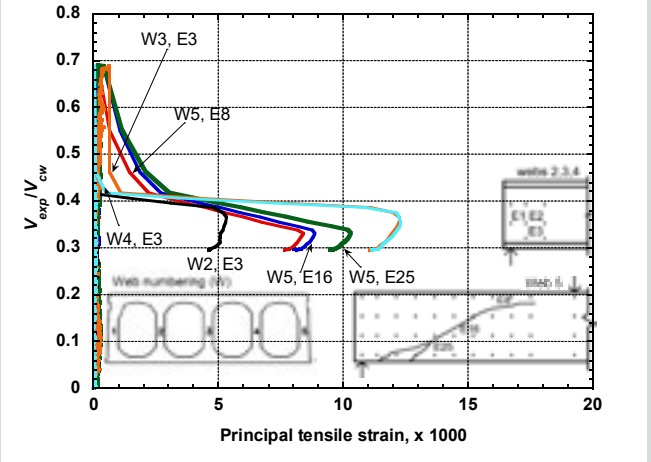

Figure 14. Principal tensile strain versus normalized applied shear for specimen 16-A1-E-3.5d. Note: V_{cw} = nominal web-cracking shear strength; V_{exp} = peak shear force applied during experiment (excluding specimen self-weight).

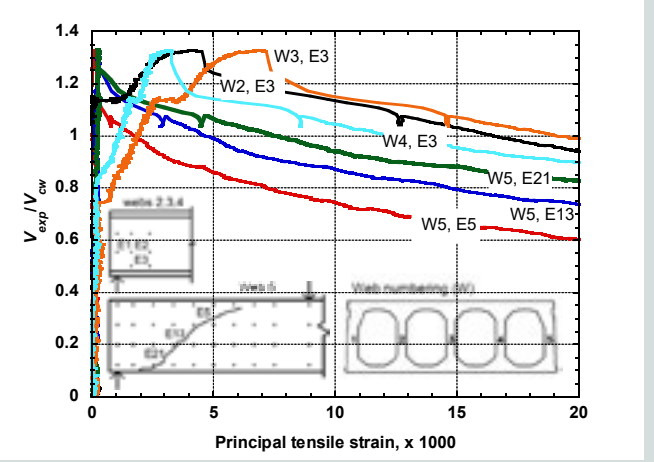

Figure 15. Principal tensile strains versus normalized applied shear for specimen 16-C1-W-3.0d. Note: V_{cw} = nominal web-cracking shear strength; V_{exp} = peak shear force applied during experiment (excluding specimen self-weight).

significant shear due to the postcracking tensile strength of fiber-reinforced concrete. The need for other webs to carry shear previously carried by the cracked web was therefore either reduced or eliminated, allowing an increase in shear beyond the first diagonal cracking. **Figure 15** shows a plot of normalized applied shear versus principal tensile strains for specimen 16-C1-W-3.0d. The interior web (W3) cracked first at an applied shear force approximately equal to the shear capacity of the 16 in. thick slabs without fibers. This crack continued to open but did not trigger a failure of the other webs. A drop in the load corresponded to the point when cracking occurred in the exterior web 5 after all interior webs had cracked.

Conclusion

Based on the experimental results and observations discussed in this paper, the following conclusions can be drawn:

- The shear strength of the two 16 in. (410 mm) thick test slabs without fibers was approximately 70% of the web-shear cracking strength V_{cw} calculated according to ACI 318-14. A substantial increase in shear strength, between approximately 55% and 90%, was obtained when hooked steel fibers were added in volume fractions of either 0.5% or 0.76% (66 or 100 lb/yd^3 [39 or 59 kg/m^3]). The shear strength exhibited by the 16 in. thick slabs with V_f equal to 0.5% was substantially greater than the calculated V_{cw}, strongly suggesting that steel fibers can be used as minimum shear reinforcement in 16 in. thick hollow-core slabs. No appreciable enhancement in behavior, however, was observed when fiber volume fraction was increased from 0.5% to 0.76%. On the contrary, problems related to concrete compaction may have a detrimental effect on shear behavior, partially offsetting the beneficial role played by fibers.

- The shear strength of the 12 in. (300 mm) thick slabs without fibers with shear span–to–depth ratio *a*/*d* of 3.0 and 3.5 was approximately 100% and 87% of the ACI 318-14 nominal web-cracking shear strength, respectively. Compared with the 16 in. (410 mm) thick slabs, the addition of steel fibers to the concrete matrix led to relatively modest increases in the shear strength of the 12 in. thick slabs (up to approximately 30%). The addition of steel fibers, however, often led to a significant increase in ductility. Consistent with the results from the tests of the 16 in. thick slabs, the increase in fiber volume fraction from 0.5% to 0.76% did not lead to any enhancement in shear strength.

- Arch action played a significant role on the behavior of the 12 in. (300 mm) thick slabs after diagonal cracking, particularly those with a shear span–to–depth ratio *a*/*d* of 3.0. This led to substantial residual strength after diagonal cracking, even in the concrete slabs without fibers. Contrary to the 12 in. thick slabs, no significant arch action was observed in the 16 in. (410 mm) thick slabs. This is attributed to the greater transfer length of the 0.6 in. diameter strands used in the 16 in. thick slabs while the support conditions remained the same.

- Overall, a good distribution of fibers was observed at the saw-cut end sections of the test slabs. Fiber counts for the slabs with V_f equal to 0.38% were consistent with the expected number of fibers calculated using the lower bound for the fiber orientation factor α of 0.41. For all other slabs except one, the counted fibers ranged between 82% and 106% of the expected number of fibers. Lower fiber counts were generally observed in the web and bottom flange, which may be an indication of a tendency of the fibers to align towards the vertical direction in these regions.

- The addition of hooked steel fibers similar to those used in this research to zero-slump concrete in volume fractions greater than 0.5% (66 lb/yd^3 [39 kg/m^3]) may lead to concrete compaction problems in hollow-core slabs, with potential detrimental effects on slab shear strength. Concrete compaction problems in test slabs with fiber volume fraction V_f of 0.76% (100 lb/yd^3 [59 kg/m^3]) translated into higher end slips and lower shear capacity compared with those in the hollow-core slabs with V_f of 0.5%. The substantial increases in shear strength obtained with the use of hooked steel fibers in a 0.5% volume fraction, combined with the compaction problems observed in slabs with higher fiber dosages, suggest that a fiber volume fraction of 0.5% may be taken as a practical upper limit for fiber content in nearly zero-slump concrete.

Acknowledgments

The research described herein was funded through a PCI Daniel P. Jenny Fellowship. Support from the U.S. Army Advanced Civil Schooling Program and the University of Wisconsin–Madison is also greatly appreciated. Thanks are also due to Mid-States Concrete Industries for the manufacturing and donation of all hollow-core slabs tested in this investigation. Bekaert Corp. kindly provided the steel fibers used in this research. The authors would also like to acknowledge the technical contributions of Professor Michael Oliva throughout this research.

References

1. Hawkins, N. M., and S. Ghosh. 2006. "Shear Strength of Hollow-Core Slabs." *PCI Journal* 51 (1): 110–115.

2. ACI (American Concrete Institute) Committee 318. 2005. *Building Code Requirements for Structural Concrete (ACI 318-05) and Commentary (ACI 318R-05)*. Farmington Hills, MI: ACI.

3. ACI Committee 318. 2014. *Building Code Requirements for Structural Concrete (ACI 318-14) and Commentary (ACI 318R-14)*. Farmington Hills, MI: ACI.

4. ACI Committee 318. 2008. *Building Code Requirements for Structural Concrete (ACI 318-08) and Commentary (ACI 318R-08).* Farmington Hills, MI: ACI.

5. Palmer, K. D., and A. E. Schultz. 2010. "Factors Affecting Web-Shear Capacity of Deep Hollow-Core Units." *PCI Journal* 55 (2): 123–146.

6. Chao, S.-H., A. E. Naaman, and G. J. Parra-Montesinos. 2009. "Bond Behavior of Reinforcing Bars in Tensile Strain-Hardening Fiber-Reinforced Cement Composites." *ACI Structural Journal* 106 (6): 897–906.

7. Baran, E., T. Akis, and S. Yesilmen. 2012. "Pull-Out Behavior of Prestressing Strands in Steel Fiber Reinforced Concrete." *Construction and Building Materials* 28 (1): 362–371.

8. MacGregor, J. G., M. A. Sozen, and C. P. Siess. 1960. *Strength and Behavior of Prestressed Beams with Web Reinforcement*. Structural research series bulletin 201. Champaign, IL: University of Illinois at Urbana-Champaign.

9. Sozen, M. A., and N. M. Hawkins. 1962. "Shear and Diagonal Tension." Discussion, *Journal of the American Concrete Institute* 59 (9): 1341–1347.

10. Olesen, S., M.A. Sozen, and C. P. Siess. 1965. *Investigation of Prestressed Concrete for Highway Bridges, Part IV: Strength in Shear of Beams with Web Reinforcement*. Engineering experiment station bulletin 49. Champaign, IL: University of Illinois at Urbana-Champaign.

11. Yang, L. 1994. "Design of Prestressed Hollow-Core Slabs with Reference to Web Shear Failure." *Journal of Structural Engineering* 120 (9): 2675–2696.

12. Parra-Montesinos, G. J. 2006. "Shear Strength of Beams with Deformed Steel Fibers." *Concrete International* 28 (11): 61–70.

13. Peaston, C., K. Elliott, and K. Paine. 1998. "Steel Fiber Reinforcement for Extruded Prestressed Hollow Core Slabs." In *SP-182: Structural Applications of Fiber Reinforced Concrete*, 87–108. Farmington Hills, MI: ACI.

14. Palmer, K. D., and A. E. Schultz. 2011. "Experimental Investigation of the Web-Shear of Deep Hollow-Core Units." *PCI Journal* 56 (4): 83–104.

15. Cuenca, E., and P. Serna. 2013. "Failure Modes and Shear Design of Prestressed Hollow Core Slabs Made of Fiber-Reinforced Concrete." *Composites Part B: Engineering* 45 (1): 952–964.

16. Simasathien, S., and Chao, S.-H. 2015. "Shear Strength of Steel-Fiber-Reinforced Deep Hollow-Core Slabs." *PCI Journal* 60 (4): 85–101.

17. ASTM Subcommittee C09.61. 2012. *Standard Test Method for Compressive Strength of Cylindrical Concrete Specimens*. ASTM C39/C39M-12a. West Conshohocken, PA: ASTM International.

18. ASTM Subcommittee C09.42. 2012. *Standard Test Method for Flexural Performance of Fiber-Reinforced Concrete (Using Beam with Third-Point Loading)*. ASTM C1609/C1609M-12. West Conshohocken, PA: ASTM International.

19. Dudnik, V. S., L. R. Milliman, and G. J. Parra-Montesinos. 2015. "Shear Strength of Prestressed Steel Fiber Reinforced Concrete Hollow-Core Slabs." Research report, University of Wisconsin–Madison.

20. Soroushian, P., and C. Lee. 1990. "Distribution and Orientation of Fibers in Steel Fiber Reinforced Concrete." *ACI Materials Journal* 87 (5): 433–439.

21. Sozen, M. A., E. M. Zwoyer, and C. Siess. 1959. *Investigation of Prestressed Concrete for Highway Bridges, Part 1: Strength in Shear of Beams Without Web Reinforcement*. Engineering experiment station bulletin 452. Champaign, IL: University of Illinois at Urbana-Champaign.

Notation

a = length of shear span

A_c = member cross-sectional area

A_f = cross-sectional area of a single fiber

A_{ps} = area of prestressing steel

b_w = web width

d = effective depth = distance from extreme compression fiber to centroid of tension steel

d_b = strand diameter

d_p = distance from extreme compression fiber to centroid of prestressing steel

f'_c = concrete compressive strength (specified strength when referring to ACI 318-14, cylinder strength when referring to test results)

f_d = stress in the concrete in the extreme precompressed fiber due to unfactored dead load

f_{pc} = compressive stress in the concrete at centroid of cross section due to effective prestressing force

f_{pe} = stress in the concrete in the extreme precompressed fiber due to the effective prestressing force

f_{pu} = ultimate strength of prestressing steel

h = member height

I = section moment of inertia

L = span length in test specimens

L_c = length of cantilever in test specimens

M_{cre} = moment due to externally applied loads

M_{max} = maximum factored moment at the section due to externally applied loads and concurrent with V_i

M_u = factored moment that occurs simultaneously with the factored shear at the section considered

N = number of fibers crossing a unit area plane

V_c = shear strength provided by the concrete

V_{ci} = nominal flexural-shear cracking strength

V_{cw} = nominal web-cracking shear strength

V_d = unfactored shear force due to dead load

V_{exp} = peak shear force applied during experiment (excluding specimen self-weight)

V_f = fiber volume fraction

V_i = factored shear force due to externally applied loads

V_p = vertical component of effective prestressing force

V_u = factored shear that occurs simultaneously with the factored moment at the section considered

y_t = distance from the centroid of the section to the extreme precompressed fiber

α = fiber orientation factor

β = angle with longitudinal axis of line connecting center of support and intersection between narrowest width of web and first critical section according to Yang's model[11]

λ = factor to account for reduced tensile strength of lightweight concrete

ρ_g = percentage of longitudinal prestressing steel based on gross area = A_{ps}/A_c

ϕ = strength reduction factor

About the authors

Vasily Dudnik, EIT, is a structural engineer at GRAEF engineering consulting firm in Madison, Wis. He received his bachelor of science and master of science degrees from the University of Wisconsin–Madison in 2013 and 2015, respectively.

Lyle R. Milliman is an instructor in the Civil and Mechanical Engineering Department at the United States Military Academy in West Point, N.Y., where he works with cadets on reinforced concrete and prestressed concrete design. He is an active duty army officer in the Army Corps of Engineers with combat deployments to Iraq and Afghanistan. He obtained his bachelor of science degree from the United States Military Academy, West Point, in 2006 and his master of science degree from the University of Wisconsin–Madison in 2015.

Gustavo J. Parra-Montesinos, PhD, is the C. K. Wang Professor of Structural Engineering at the University of Wisconsin–Madison. He is member of the American Concrete Institute (ACI) Committee 318, Structural Concrete Building Code, and chair of ACI 318-J, Joints and Connections. He is also chair of joint ACI-ASCE Committee 352, Joints and Connections in Monolithic Concrete Structures, and member of joint ACI–American Society of Civil Engineers (ASCE) Committee 335, Composite and Hybrid Structures, and of *fib* (International Federation for Structural Concrete) T4.1, Fibre-Reinforced Concrete. His research interests include the behavior and design of reinforced/prestressed concrete, fiber-reinforced concrete, and hybrid steel-concrete structures.

Abstract

An experimental study was conducted to evaluate the effect of steel fibers on the shear strength of prestressed concrete hollow-core slabs. The main variables investigated were fiber volume fraction (0.38%, 0.5%, and 0.76%), slab thickness (12 and 16 in. [300 and 410 mm]), and shear span–to–depth ratio (3.0 and 3.5). The addition of steel fibers to 16 in. thick hollow-core slabs led to an increase in shear strength between approximately 55% and 90% compared with that of regular (no fibers) concrete hollow-core slabs. Furthermore, the 16 in. thick slabs with fiber volume fractions of 0.5% and 0.76% exhibited shear capacities above the nominal web-cracking shear strength calculated according to ACI 318-14. Alternatively, steel fibers led only to a relatively modest improvement, up to 30%, in the shear capacity of 12 in. thick slabs. The behavior of these slabs was significantly influenced by arch action, which led to substantial residual strength after diagonal cracking, regardless of the presence of fibers.

Keywords

Diagonal cracking, hooked steel fibers, shear reinforcement, shear strength, tensile strength, web cracking.

Review policy

This paper was reviewed in accordance with the Precast/Prestressed Concrete Institute's peer-review process.

Reader comments

Please address reader comments to journal@pci.org or Precast/Prestressed Concrete Institute, c/o *PCI Journal*, 200 W. Adams St., Suite 2100, Chicago, IL 60606.